Aquaculture 559 (2022) 738420

Contents lists available at ScienceDirect

Aquaculture

journal homepage: www.elsevier.com/locate/aquaculture

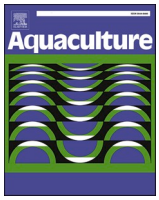

Knockout of Hermansky-Pudlak Syndrome 4 (*hps4*) leads to silver-white tilapia lacking melanosomes

Chenxu Wang [a], Thomas D. Kocher [b], Baoyue Lu [a], Jia Xu [a], Deshou Wang [a,*]

[a] *Key Laboratory of Freshwater Fish Reproduction and Development (Ministry of Education), Key Laboratory of Aquatic Science of Chongqing, School of Life Sciences, Southwest University, Chongqing 400715, China*
[b] *Department of Biology, University of Maryland, College Park, MD 20742, USA*

ARTICLE INFO

Keywords:
hps4 mutation
CRISPR/Cas9
Melanin
Pigment cells
Silver-white body color
Tilapia

ABSTRACT

Body color is a major factor determining the economic value of farmed tilapia. In the present study, we engineered a silver-white tilapia by mutation of *hps4* using CRISPR/Cas9 gene editing of a target site in exon 2. Homozygous mutation of *hps4* led to a truncated protein of only 80 amino acids. Disruption of HPS4 led to a significant decrease (even absence at the adult stage) of melanophores and melanin, and a significant increase of iridophores, xanthophores and erythrophores. A sub-group of melanophores, even though very few in number, was found in the early embryonic stages. White iridophores without iridescence, hypertrophic xanthophores, and erythrophores with plenty of pigments were detected in the scales and caudal fins of the mutants, indicating enrichment of guanine, pteridine and carotenoids. To our knowledge, this is the first report on disruption of HPS4 in teleosts, and the first report demonstrating that HPS4 regulates iridophore, xanthophore and erythrophore numbers. *Hps4* plays a fundamental role in LROs (lysosome-related organelles) -pigment development, melanophore survival and melanin biosynthesis. Our *hps4* mutants provide a new model for studies of HPS4 function in vertebrates, and might be used as new germplasm for aquaculture.

1. Introduction

It is well known that body color and color pattern play an important role in survival, reproduction, behavior, and prevention of skin cancer in vertebrates (Hoekstra, 2006; Protas and Patel, 2008; Sköld et al., 2016). Additionally, body color is also an important economic trait in domesticated animals. Many studies have been conducted to improve the color traits of domesticated animals, including cross-breeding, supplementation with carotenoid-rich food, and recently gene editing. Many pleasant body color mutants have been created, and are favored by customers. Fish is an important protein resources for human, and customers associate body color with meat quality, and nutritional value (Lehnert et al., 2019; Maoka, 2020; Wu et al., 2022). Thus improving color traits is a priority. Even though many studies have been conducted to improve the color traits of food fish (Chen et al., 2018; Xu et al., 2015; Wang et al., 2022; Liu et al., 2019), this research still lags behind that for other domesticated animals.

As the most common pigment cell type in animals, melanophores have been studied for over 150 years, and more than 200 genes have been found to affect melanoblast migration, melanophore differentiation, survival and melanin biosynthesis (Yamaguchi and Hearing, 2009; Ito and Wakamatsu, 2011). Most of the melanophore-related studies were conducted in humans, mice, chicken, African frogs, medaka, and zebrafish, and the majority of the research was conducted on the well-known cAMP/CREB-*mitf* axis and tyrosinase metabolism pathways. Many genes in these pathways, like *mitf*, *tyr*, *dct*, *pmel,* have been acknowledged to be fundamental for directing melanophore survival and melanogenesis (Hou and Pavan, 2008). The role of *hps* gene family members in melanogenesis is less known. A total of nine human HPS (Hermansky-Pudlak syndrome)-causing genes have been identified, each of which corresponds to a different HPS subtype. Some genes in the family have been shown to traffic melanogenic enzymes tyrosinase (Tyr), tyrosinase-related protein 1 (Tyrp1), and tyrosinase-related protein 2 (Tyrp2), from the Golgi to the developing melanosome (Raposo

Abbreviations: CRISPR/Cas9, clustered regularly interspaced short palindromic repeats/CRISPR associated protein 9; HPS4, Hermansky-Pudlak syndrome 4 protein; RPE, retinal pigment epithelium; LROs, lysosome-related organelles; MITF, melanocyte-inducing transcription factor; NCCs, neural crest cells; NCBI, National Center for Biotechnology Information.

* Corresponding author.
E-mail address: wdeshou@swu.edu.cn (D. Wang).

https://doi.org/10.1016/j.aquaculture.2022.738420
Received 22 April 2022; Received in revised form 23 May 2022; Accepted 25 May 2022
Available online 30 May 2022

et al., 2001; Huizing et al., 2004, 2008; Daly et al., 2013). Additionally, nine HPS genes have been identified in mouse by mapping and mutation (Wei, 2006). HPS4 is part of BLOC3 (biogenesis of lysosome-related organelles complex 3) which is involved in trafficking of melanosome cargo from the Golgi to stage III melanosomes (Wasmeier et al., 2008; Gerondopoulos et al., 2012). Lack of BLOC3 has been found to lead to accumulation of stage I melanosomes and the decrease of phase IV melanosomes (Nguyen et al., 2002; Gerondopoulos et al., 2012).

Studies on the *hps* family in teleosts are rare. *hps4* has been confirmed to be fundamental for channel catfish body color variation through GWAS (Genome-wide association study) mapping, in which a natural mutation of the *hps4* allele leads to completely albino fish (Li et al., 2017). In mice, disruption of the HPS family, including HPS4, leads to melanophore deficiency. However, to our knowledge, no loss of function study of *hps4* has been conducted in any vertebrate except for mice.

The specific composition and distribution of pigment cells is a major contributor to the body color and color pattern of animals. Mammals and birds contain only one kind of pigment cell (melanocytes), but lower vertebrates like fish have additional types of pigment cells including xanthophores, iridophores, erythrophores, leucophores and cyanophores (Fujii, 2000; Kelsh, 2004; Sköld et al., 2016). Fish have rich and dazzling pigment patterns composed of these different pigment cell types, which make them ideal for studying the developmental basis of body coloration (Patterson and Parichy, 2019).

Several studies have suggested that cichlids are a useful model for studying the formation of vertebrate body color (Kocher, 2004; O'Quin et al., 2013; Santos et al., 2014; Kratochwil et al., 2018; Hendrick et al., 2019; Liang et al., 2020). Several loss of function studies have been conducted in recent years (Kratochwil et al., 2018; Wang et al., 2021; Lu et al., 2022; Li et al., 2021; Segev-Hadar et al., 2021; Pandey et al., 2021). Tilapias are an important aquaculture species world-wide. The Nile tilapia is the most popular aquaculture species, and is an excellent model for study teleosts body color formation (Wang et al., 2021). In this study, we engineered a silver-white tilapia strain and characterized its phenotype by quantifying pigment cell numbers, cell sizes and the total melanin content at different developmental stages.

2. Materials and methods

2.1. Fish

The founder strain of Nile tilapia was obtained from Prof. Nagahama (Laboratory of Reproductive Biology, National Institute for Basic Biology, Okazaki, Japan). Experimental tilapia were reared in recirculating aerated freshwater tanks and maintained at ambient temperature (27 °C) under a natural photoperiod. Prior to the experiments, the fish were kept in laboratory aquariums under 15:9 h light: dark conditions at a temperature of 27 ± 1 °C for one week. All animal experiments conformed to the Guide for the Care and Use of Laboratory Animals and were approved by the Committee for Laboratory Animal Experimentation at Southwest University, China.

2.2. The expression level analysis of hps4 in different tissues

The expression levels of *hps4* in different tissues of Nile tilapia were downloaded from NCBI database (Brawand et al., 2014).

2.3. The gene functional domain prediction and promoter binding sites analysis

The complete amino acid sequence of *hps4* in Nile tilapia was downloaded from the NCBI database (with GenBank accession number 100709428) and functional domain prediction carried out using SMART (http://smart.embl-heidelberg.de/). The 2kbp promoter sequences of *hps4* were downloaded from the NCBI database. The *cis*-regulating elements of the promoter were predicted using the AnimalTFDB3.0 program (http://bioinfo.life.hust.edu.cn/AnimalTFDB/#!/tfbs_predict), and the MITF binding consensus sequences were highlighted.

2.4. Establishment of $hps4^{-/-}$ mutants by CRISPR/Cas9

CRISPR/Cas9 was performed to knockout *hps4* in tilapia as described previously (Wang et al., 2021). Briefly, the guide RNA and Cas9 mRNA were co-injected into one-cell-stage embryos at a concentration of 150 and 500 ng/μL, respectively. About 400 fertilized eggs were used for gene editing and 100 for control. Twenty injected embryos were collected 72 h after injection. Genomic DNA was extracted from pooled control and injected embryos and used to characterize the mutations. DNA fragments spanning the target site was amplified. The gene-specific sequences were listed in Table S1. The mutated sequences were analyzed by restriction enzyme digestion with *Nco*I and Sanger sequencing.

The *hps4* mutant fish with the highest indel frequency were used as F0 founders. Heterozygous F1 offspring were obtained by crossing F0 XY male founders to WT XX females. F1 larvae were collected at 10 dah (days after hatching) and genotyped by PCR amplification and subsequent *Nco*I digestion. The F1 fish were genotyped by fin clip assay and the individuals with frame-shift mutations were selected. XY male and XX female siblings of the F1 generation, carrying the same mutation, were mated to generate homozygous F2 mutants. The $hps4^{-/-}$ mutants were screened using restriction enzyme digestion and Sanger sequencing. The genetic sex of each fish was determined by genotyping using sex-linked marker (Marker 5) as described previously (Sun et al., 2014).

2.5. Image recording and pigment cell observation of the mutants and wild-type fish

Larvae (3, 5, and 7 dpf) submerged in clean water were photographed from the lateral view by Olympus SZX16 stereomicroscope (Olympus, Japan) under bright field. Larval fish at 12 dpf and 30 dpf were first anesthetized with tricaine methasulfonate (MS-222, Sigma-Aldrich, USA), then shifted to an observation dish with clean water, photographed from the lateral view by Olympus SZX16 stereomicroscope (Olympus, Japan) under bright field and transparent field with various magnification. The 150 dpf, 6 months (180 dpf) and 19 month (570 dpf) aged adult wild-type and mutant fish were shifted to 30 × 5 × 20 cm^3 glass water tanks, before being photographed with a Nikon D7000 digital camera (Nikon, Japan) against a blue background. The caudal fins of fish at 150 dpf were removed with medical scissors, soaked in 0.65% Ringers' solution and directly observed with Olympus SZX16 stereomicroscope without cover slip under transparent or bright field. Scales of fish at 6 months and 19 months stage were soaked in 0.65% Ringers' solution under cover slip, and were observed under Leica EM UC7 microscope (Leica, Germany). To analyze the number of melanophores and xanthophores, 5 mutants and 5 wild-type fish were anesthetized with tricaine methasulfonate (MS-222, Sigma-Aldrich, USA) and immersed in 10 mg/ml epinephrine (Sigma, USA) solution for 15 min to contract melanin and erythrosome. Image recording of pigment cells were conducted as quickly as possible after putting them in the Ringers' solution as the preparations are not stable. The sizes of the melanophores and relative iridophore content were measured using Image J software (Schneider et al., 2012). ACDSee Official Edition software (ACDSystems, Canada) and Adobe Illustrator CS6 (Adobe Inc. USA) were used to format the pictures.

2.6. Melanin quantification and melanin biosynthesis abilities comparison

To analyze the number of melanophores, three fish per group were anesthetized with tricaine methasulfonate (MS-222, Sigma-Aldrich, USA). Skin sample suspensions were solubilized in 8 M urea/1 M sodium hydroxide and cleared by centrifugation at 10,700*g* for 10 min. Chloroform was added to the supernatants to remove fatty impurities.

Skin samples containing pheomelanin were cleared by centrifugation at 10,700*g* for 10 min and analyzed for absorbance at 400 nm (Dong et al., 2012; Yan et al., 2013).

2.7. Data analysis

Data are expressed as mean ± SD. GraphPad Prism 5.01 software (Graphpad, USA) was used to analyze and export the differences in the numbers and sizes of melanophores and the melanin content in *hps4*$^{-/-}$ mutants and wild type fish. Differences in the data between wild-type and mutants were tested by two-tailed Student's *t*-test (***, $P < 0.001$; **, $P < 0.01$; *, $P < 0.05$; ns, not significant).

3. Results

3.1. Gene structure and functional domain of hps4/HPS4 in Nile tilapia

The Nile tilapia *hps4* gene has 12 exons and 11 introns (Fig. 1A). The binding sites predicted by Animal TFDB 3.0 suggested that there are three *mitf* binding sites in the promoter regions of *hps4*, indicating that *hps4* is probably regulated by *mitf* (Fig. S1). Additionally, functional domain predicted by SMART showed that there are seven low complexity regions in the amino acid sequence, and these regions might be necessary for the basic functions of HPS4 (Fig. 1F, indicated by green boxes).

3.2. Establishment of the hps4$^{-/-}$ mutant line in tilapia

Similar to the expression patterns of all the *hps* family members in mice and humans, *hps4* also ubiquitously expressed in many tissues of tilapia, even though the expression levels were not very high (Fig. S2). To disrupt tilapia *hps4* we targeted a site in exon 2 with CRISPR-cas9. *Nco*I was used for enzymatic digestion of the amplified target regions. The sequences of gRNA target was CCGGCGTGGGCCGCTGCGTCTCC, in which CCG were used as the PAM region (Fig. 1A and C). F0 founders were screened by restriction enzyme digestion and Sanger sequencing (Fig. 1B and C). In the *hps4* F0 chimeras, various levels of hypo-pigmentation were observed in body, and the eyes (RPE and iris) were also hypo-pigmented, both in early embryonic developmental stage (Fig. S3) and adult stage (Wang et al., 2021). The eyes in some of the mutants (F0) showed unilateral and bilateral hypo-pigmentation (red), while the majority showed black eyes like the wild-type fish. These results indicate that *hps4* is fundamental for body color formation and eye pigmentation in tilapia, and is probably necessary for melanin synthesis in all melanophores (neural crest cells, NCCs-derived and optic-cup-derived melanophores). The *hps4* mutant fish with a high mutation rate (over 75%) raised to sexual maturity and mated with wild-type tilapia to create F1 fish. Heterozygous *hps4* F1 offspring with a − 7 bp deletion in the fourth exon were selected to breed the F2 generation (Fig. 1D and E).

3.3. Melanophores were significantly decreased in the yolk sac and body of mutants at 3, 5 and 7 dpf

Melanophores first appeared on the yolk sac at 27.5 hpf (hours post fertilization), and rapidly increased at 3 dpf (Wang et al., 2021). The wild-type fish had many pigmented melanophores on the yolk sac, a few melanophores on the top head, and a few melanophores and iridophores in the iris, but no melanin were detected in the RPE at 3 dpf (Fig. 2A). At 5dpf, many melanophores/melanin were detected on the yolk sac and RPE, and the iris was filled with iridophores and melanophores (Fig. 2B). At 7dpf, many melanophores were detected on the yolk sac, top head, trunk and RPE (melanin). The majority of melanophores were macro-melanophores on the top of the head (Fig. 2C).

In contrast, no pigmented melanophores were detected in the *hps4*$^{-/-}$ mutants at 3 or 5 dpf. Many iridophore-composed white spots (iridophores rich in lysosome) were detected in the head and along the dorsal trunk at 3 dpf, suggesting that the iridophores could be observed

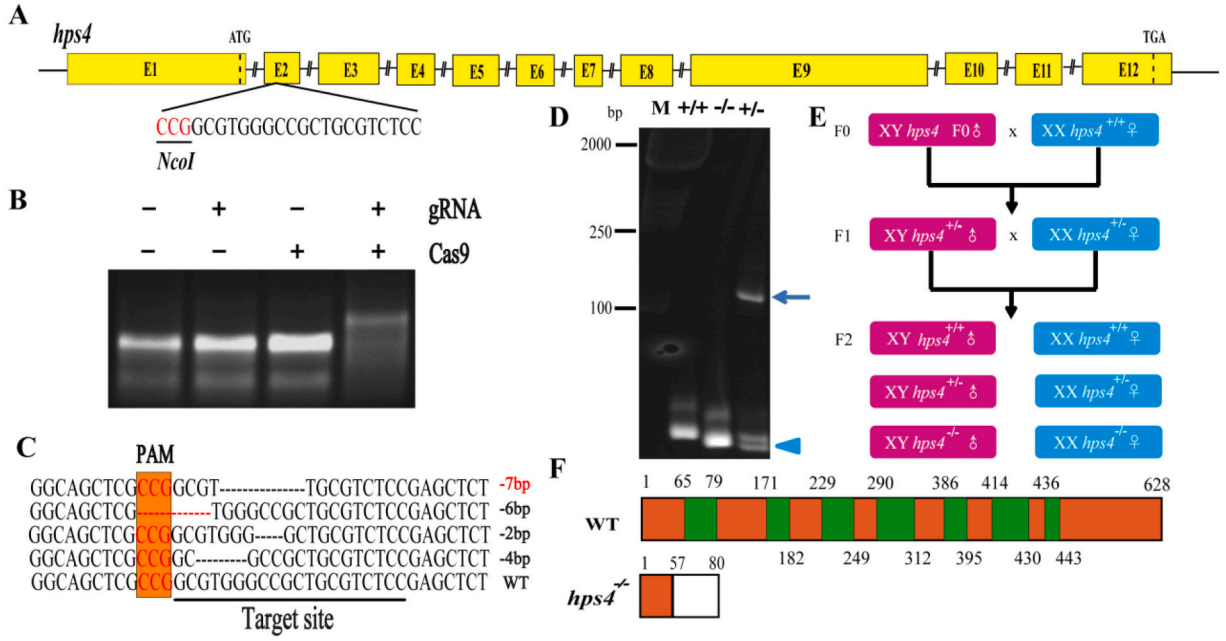

Fig. 1. Establishment of *hps4*$^{-/-}$ (A–F) mutant line in Nile tilapia.
A: Gene structures of *hps4* showing the target site and the *Nco*I restriction site. B: Restriction enzyme digestion of the amplified fragment of *hps4* using primers spanning the target sites. The Cas9 mRNA and gRNA were added as indicated. C: Sanger sequencing results from the uncleaved bands were listed. The PAM is marked in orange. Deletions are marked by dashes (−) and numbers to the right of the sequences indicate the loss of bases for each allele. WT, wild type. D: Identification of *hps4* F2 genotypes by hetero-duplex motility assay. Arrowheads show homo-duplexes and arrows show hetero-duplexes. E: Schematic diagram showing the breeding plans of *hps4* F0 to F2 fish. F: Tilapia HPS4 intact (with seven low complicity regions, green box) and mutated protein. Mutation of *hps4* resulted in a truncated protein composed of 56 amino acids. (For interpretation of the references to color in this figure legend, the reader is referred to the web version of this article.)

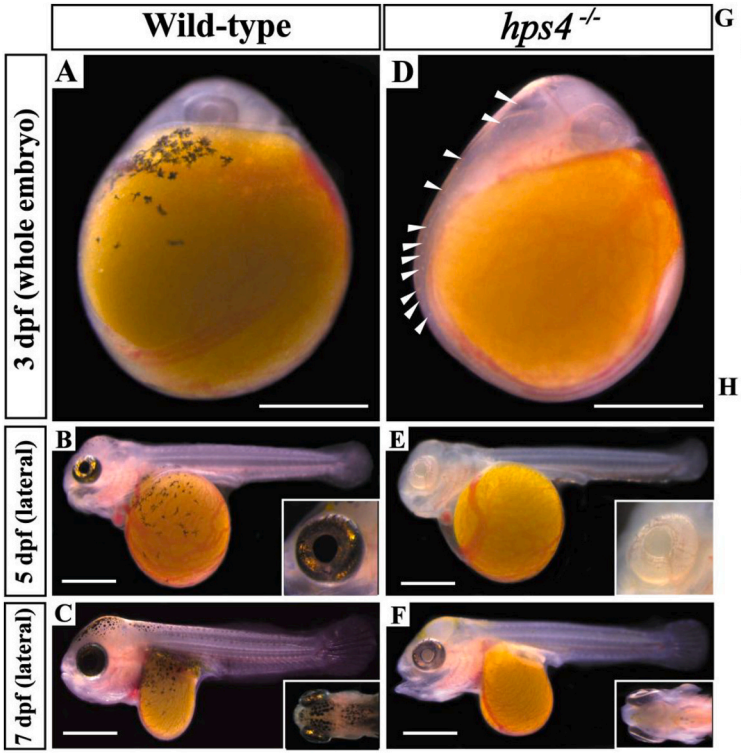

Fig. 2. Melanophores were significantly decreased in yolk sac and body of the mutants at 3, 5 and 7 dpf. A–C: Wild-type fish. Many melanophores on the yolk sac, a few on the iris were detected, while no melanin was detected in the RPE at 3 dpf (A). Increased melanophores were detected on the yolk sac. The RPE was filled with melanin and the iris was filled with iridophores and melanophores at 5 dpf (B). Further increased melanophores were detected on the yolk sac, the top head (mainly covered by macro-melanophores) and the trunk, and increased melanin was detected in the RPE at 7 dpf (C). D-F: *hps4*$^{-/-}$ mutants. No pigmented melanophores were detected in the whole embryo, while many white iridophore-composed spots (white arrow heads) were detected in the head and trunk of the mutants at 3 dpf (D). No pigmented melanophores were detected in the whole embryo, while vast increase of iridophores was observed in the iris. At the same time, apparent capillary network was detected on the iris of the mutants at 5 dpf (E). Several pigmented melanophores appeared in the top head, while no pigmented melanophores were detected in the yolk sac and lateral trunk. Besides, the RPE still showed no melanin, the iris showed some pigmented melanophores and many iridophores in the mutants at 7 dpf (F). G, H: Quantification of white pigment cell spots in the whole embryo and melanophores in the head at 3 dpf and 7 dpf, respectively. White pigment cell spots in mutants were significantly higher than those in wild-type fish at 3 dpf (G). Melanophore numbers in the head of wild-type fish were significantly higher than those in mutants at 7 dpf (H). Data in G and H are expressed as mean ± SD (n = 5). Differences in the data between wild-type and mutants were tested by two-tailed Student's t-test, ***$P < 0.001$, **$P < 0.01$, *$P < 0.05$, ns: not significant. A-F, 1 mm.

through the overlying unpigmented melanophores in the mutants (Fig. 2D). Many iridophores were detected in the iris at 5 dpf (Fig. 2E). At 7 dpf, several melanophores were appeared in the top head while melanophores were still not detected on the yolk sac or lateral trunk. Additionally, even though no melanin was detected in the RPE, some melanophores and many iridophores were detected in the iris (Fig. 2F). The *hps4*$^{-/-}$ mutants showed obvious hypo-pigmentation from the early embryonic stages.

Quantification of the pigment cells revealed significantly higher number of iridophores at 3 dpf, and significantly lower number of pigmented melanophores on top head at 7 dpf in *hps4*$^{-/-}$ mutants than in wild-type fish (Fig. 2G and H).

3.4. Melanophores were significantly decreased in number and size on head and eye and completely lost in body of the mutants at 12 dpf

Both bright and transparent fields were used to analyze the pigment cells and color patterning of fish at 12 dpf. Many melanophores in head, eyes and the trunk were detected in the wild-type fish. The melanophores were spread evenly in the trunk as it was within the time period after the disappearance of yolk sac but before the formation of the bars and inter-bars. In addition, many iridophores were detected in the peritoneum, followed by the operculum and iris (Fig. 3A). Under higher magnification, the majority of melanophores on the head were "macro-melanophores" with sizes larger than the melanophores on the trunk. A few iridophores neighboring the macro-melanophores or attached on the main body of the melanophores, and a few xanthophores in the gap between the melanophores were also detected on the head (Fig. 3B). The eyes had a heavily pigmented black RPE and an iridescent-black iris composed of many melanophores and iridophores (Fig. 3C).

In contrast, almost no melanophores were detected in the *hps4*$^{-/-}$ mutants, while iridophores were present in large numbers. The peritoneum was less transparent than earlier stages as the number of iridophores greatly increased (Fig. 3D and E). Only a few fragmented small melanophores were observed on the head. Almost no black pigmentation was observed in the RPE, which displayed a pink-yellow color due to blood capillaries. The iris contained excessive iridophores like the trunk (Fig. 3F).

Quantification of the pigment cells revealed significantly lower number and size of melanophores on the head and also significantly lower relative melanin content in the iris (Fig. 3G, H and J), but significantly higher relative iridophore content on top of the head in *hps4*$^{-/-}$ mutants than in wild-type fish at 12 dpf (Fig. 3I).

3.5. Significantly decreased melanophores and increased iridophores in trunk and eye of mutants at 30 dpf

Thirty dpf is the key time point for the formation of vertical bars during metamorphosis in wild-type fish, in which a higher density of melanophores and more large sized melanophores appear in the bar than in the inter-bar (Fig. 4A). Many widely spread iridophores and xanthophores were detected in both the bars and inter-bars (Fig. 4B). The RPE was black with abundant melanin, while many melanophores and iridophores were detected in the iris (Fig. 4C).

In *hps4*$^{-/-}$ mutants, no pigmented melanophores or melanin were present, hence the fish displayed a uniform silver-white body color (Fig. 4D). Many iridophores gathered as big spots, which gave a strong iridescence in the skin and scales (Fig. 4E). The RPE displayed a dark red color, due to increased capillaries and carotenoid pigment. The iris was silver-white with some carotenoid-derived reddish color patterning (Fig. 4F).

Quantification of the pigment cells revealed significantly lower

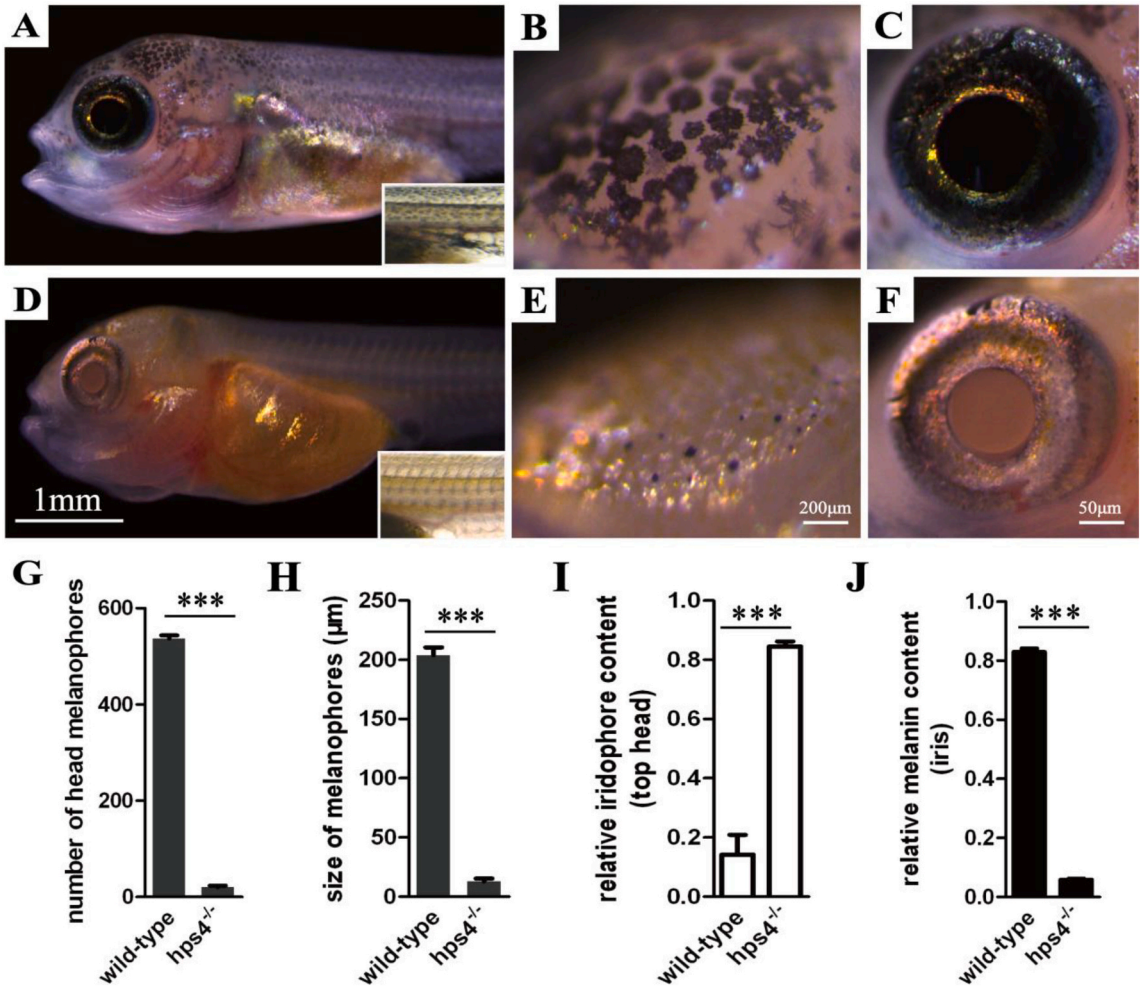

Fig. 3. Melanophores were significantly decreased in number and size in head and iris and completely lost in body of the mutants at 12 dpf.
A–C: Wild-type fish. Many evenly distributed melanophores were detected in the trunk and iris. The RPE was black, and the iris was detected with many melanophores and iridophores (A). Higher magnification of the top head showing the macro-melanophores and iridophores (B). Dark melanin was observed in the RPE, and many melanophores and iridophores were observed in the iris (C). D-F: *hps4*$^{-/-}$ mutants. Serious hypo-pigmentation was detected, with a few small-sized melanophores in the head and absence of pigmented melanophores in the trunk, RPE (melanin) and fins. In contrast, significantly increased iridophores were observed in the whole fish (D). Higher magnification of the top head showing a few small sized melanophores and significantly increased iridophores (E). The RPE was pink-yellowish, due to the absence of melanin. The iris was fulfilled with iridophores and a few pigmented melanophores (F). G, H: Quantitative analysis of the numbers and sizes of the melanophores in the head of the mutants and wild-type fish, respectively. I, J: Quantitative analysis of the relative iridophore and melanin content in the top head and iris, respectively. Data in G-J are expressed as mean ± SD ($n = 5$). Differences in the data between wild-type and mutants were tested by two-tailed Student's *t*-test, ***$P < 0.001$, **$P < 0.01$, *$P < 0.05$, ns: not significant. (For interpretation of the references to color in this figure legend, the reader is referred to the web version of this article.)

number of melanophores, while significantly higher relative iridophore content in the skin of *hps4*$^{-/-}$ mutants than in wild-type fish at 30 dpf (Fig. 4G–4J).

3.6. Significantly increased iridophores were observed in the ventral skin and scales of *hps4*$^{-/-}$ mutants at 30 dpf

Under bright field, the wild-type fish and *hps4*$^{-/-}$ mutants showed a strong iridescent color in skin and scales. The iridescent signal in wild-type ventral skin was stronger than the dorsal trunk, which was in consistent with dorsal-ventral counter shading in vertebrates. The *hps4*$^{-/-}$ mutants displayed a stronger iridescence in the skin and scales than the wild-type fish due to more iridophores (Fig. 5A and B). In contrast with the wild-type fish, the dorsal-ventral counter shading was disrupted in the mutants. Quantification analysis revealed significantly higher relative iridophore contents in ventral skin of *hps4*$^{-/-}$ mutants than in wild-type fish at 30 dpf (Fig. 5G–5J).

3.7. Significantly increased iridophores, xanthophores/erythrophores, but no pigmented melanophores/melanin, were observed in trunk, RPE, iris, fins and scales of mutants at 150 dpf

At 150 dpf, the wild-type fish had stable vertical bars and inter-bars (Fig. 6A). The RPE and the iris were black (Fig. 6C). The fins and scales were pigmented with many melanophores, many xanthophores distributed in the gap between bars, and many iridophores gathered in spots (Fig. 6D, D' and 6E).

In contrast, the *hps4*$^{-/-}$ mutants displayed a strong silver-white body color, without bars and inter-bars due to the absence of pigmented melanophores and increased numbers of iridophores (Fig. 6B). The RPE became dark red with increased carotenoids pigment. The iris was basically silver-white but with some carotenoids-derived reddish pigmentation (Fig. 6F). Many xanthophores (projecting "airenemes" in the scales) and white iridophores, but no melanophores, were detected in fins (Fig. 6G and G') and scales (Fig. 6H). Increased numbers of erythrophores were also observed in the fins of the mutants compared

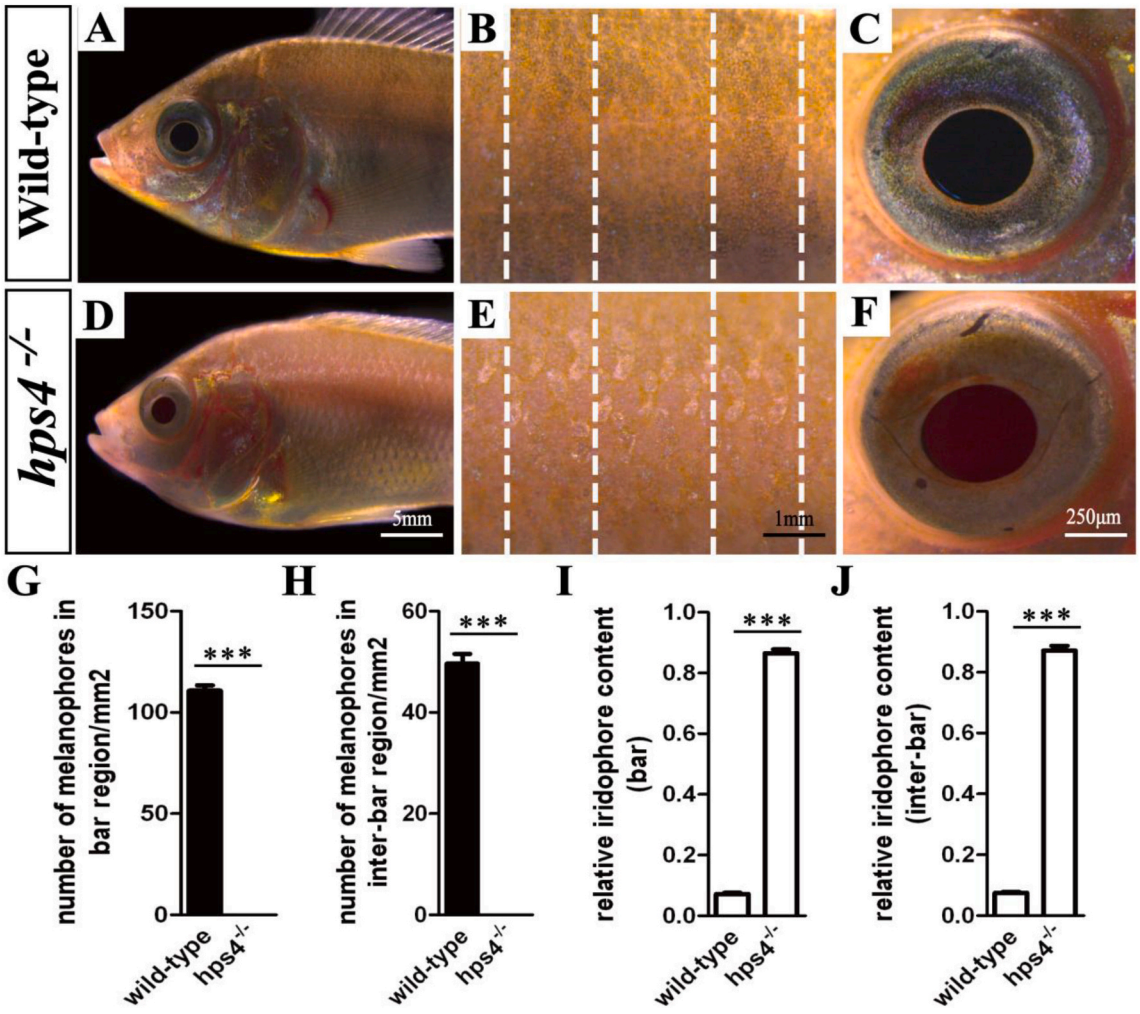

Fig. 4. Significantly decreased melanophores and increased iridophores were observed in the trunk and eye of the mutants at 30 dpf.
A–C: In the wild-type fish, the trunk was detected with many melanophores with higher densities in the dark bars than in the light inter-bars, and many iridophores spread in both the bars and inter-bars (A, B). The RPE was fulfilled with melanin, and the iris was detected with many iridophores and xanthophores (C). D–F: In the *hps4*$^{-/-}$ mutants, serious hypo-pigmentation was detected. No pigmented melanophores, but increasing reddish coloration, were detected in the trunk, fin and iris. In contrast, significantly increased iridophores were detected in both skin and scales (D, E). No melanin was observed in the RPE which displayed dark red color. Significantly increased iridophores and red coloration were detected in the iris, similar to the body (F). G, H: Quantitative analysis of the numbers of the melanophores in the bar and inter-bar regions of the mutants and wild-type fish. I, J: Quantitative analysis of the relative iridophore content in the bar and inter-bar regions of the mutants and wild-type fish. Data in G–J are expressed as mean ± SD ($n = 5$). Differences in the data between the mutants and wild-type were tested by two-tailed Student's *t*-test, ***$P < 0.001$, **$P < 0.01$, *$P < 0.05$, ns: not significant. (For interpretation of the references to color in this figure legend, the reader is referred to the web version of this article.)

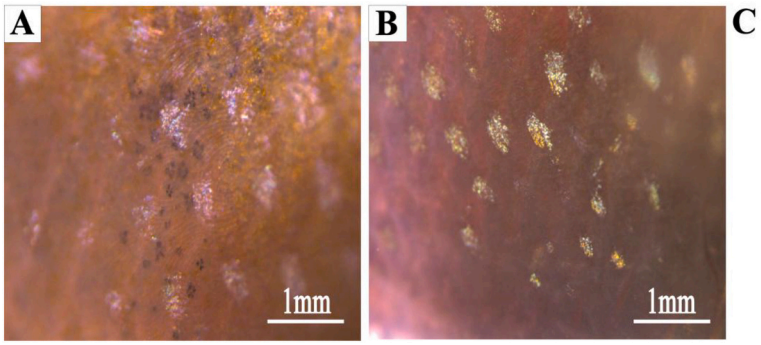

Fig. 5. Significantly increased iridophores were observed in the ventral skin and scales of the *hps4*$^{-/-}$ mutants at 30 dpf.
A: In wild-type fish, the ventral skin was detected with many iridophores and some melanophores. The iridophores gathered in big spots on the scales gave a strong iridescent color in the area. B: In the *hps4*$^{-/-}$ mutants, the ventral skin was detected with many iridophore-composed big spots covering the scales. C: Significant higher relative iridophore content was detected in the mutants than in the wild-type fish. Data in C are expressed as mean ± SD (n = 5). Differences in the data between groups were tested by two-tailed Student's *t*-test, ***$P < 0.001$, **$P < 0.01$, *$P < 0.05$, ns: not significant.

with the wild-type fish.

Quantification of the pigment cells revealed significantly lower number of melanophores in caudal fin and dorsal scales, while significantly higher relative iridophore content and erythrophore/xanthophore numbers in caudal fin of *hps4*$^{-/-}$ mutants than in wild-type fish at 150 dpf (Fig. 4I–4L). In consistent, melanin content was very

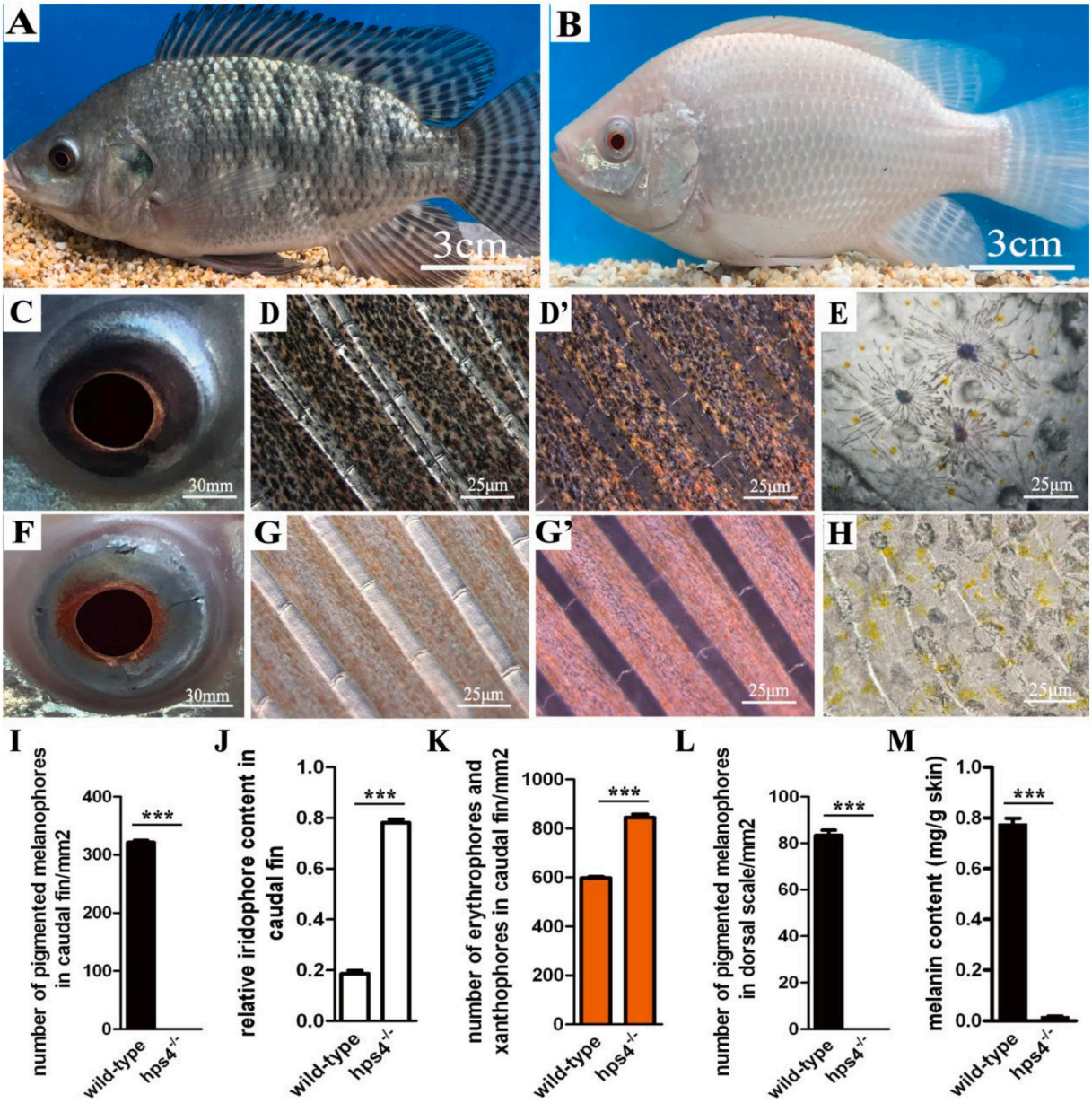

Fig. 6. Significantly increased iridophores, erythrophores/xanthophores and no melanophores/melanin were observed in the trunk, RPE, iris, fins and scales of the mutants at 150 dpf.

A, C, D, D′ and E: The wild-type fish displayed dark bars separated by light inter-bars in the trunk and fins. The RPE was heavily pigmented, and the iris showed many melanophores. The caudal fin and scales showed many melanophores and xanthophores. B, F, G, G' and H: The *hps4*$^{-/-}$ mutants displayed dark red RPE and silver-white body with no bars in the trunk and fins due to the absence of pigmented melanophores/melanin. The fins showed significantly higher relative iridophore content, and a higher number of erythrophores/xanthophores, compared with the wild-type fish. Scales were filled with increased white iridophores and dispersed xanthophores. I-K: Quantitative analysis of the numbers of the pigmented melanophores, relative iridophore content and number of erythrophores/xanthophores in the caudal fins of the mutants and wild-type fish. L: Quantitative analysis of the numbers of the pigmented melanophores in the dorsal scales of the mutants and wild-type fish. M: Quantification of the melanin content in the dorsal skin. Abundant melanin was detected in the wild-type fish, while almost no melanin was detected in the mutants. Data in I-M are expressed as mean ± SD (n = 5). Differences in the data between the wild-type fish and mutants were tested by two-tailed Student's *t*-test, ***$P < 0.001$, **$P < 0.01$, *$P < 0.05$, ns: not significant. (For interpretation of the references to color in this figure legend, the reader is referred to the web version of this article.)

high (0.78 mg/g skin) in the wild-type fish, while almost no melanin was detected in the mutants (Fig. 6M).

3.8. Increased xanthophores/erythrophores in trunk and fins and iridophore spots in scales were observed in *hps4*$^{-/-}$ mutants at 6 and 19 months

Different from the wild-type fish (Fig. 7A and A'), an obvious increase of reddish coloration, due to increased erythrophores in red spots, were detected in whole trunk, fins, RPE and iris in the *hps4*$^{-/-}$ mutants at 19 months (Fig. 7B and B'). Additionally, the mutants were still detected with some banding in the dorsal, anal and caudal fins (Fig. 7B and Fig. S4), suggesting that melanophores were probably there, while just not pigmented.

Under bright and transparent field, no erythrophores were observed in scales of either the wild-type fish or the mutants at 6 months (Fig. 8A,

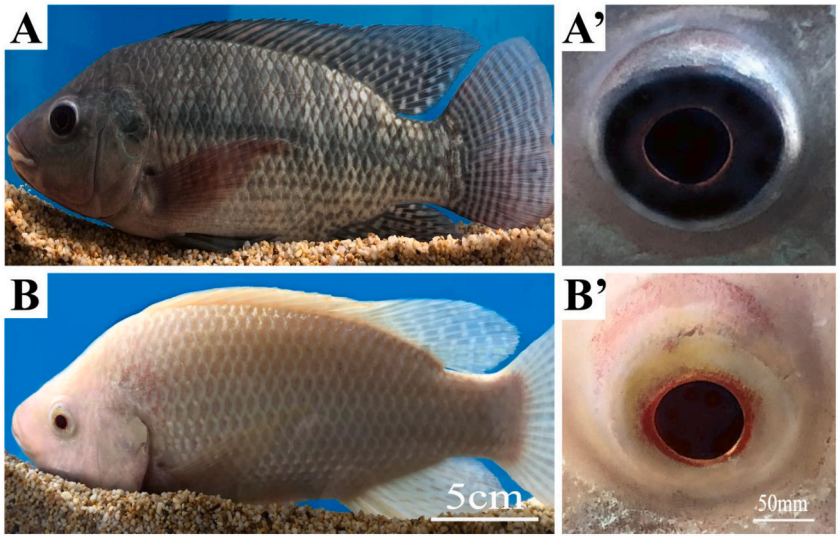

Fig. 7. Obvious reddish-silver-white color patterning was observed in mutants at 19 months.
A and A': The wild-type fish showed black body color, while the caudal fin and pectoral fins showed reddish color patterning. The iris was filled with melanophores and the RPE was heavily pigmented with melanin. B and B′: The *hps4*$^{-/-}$ mutants showed a global reddish-silver-white body color. No pigmented melanophores were detected in the whole fish. The iris showed a yellow-white color, with reddish pigmentation around the RPE. The RPE was dark red. (For interpretation of the references to color in this figure legend, the reader is referred to the web version of this article.)

A', 8B and 8B'). Increased iridophores and xanthophores were observed in the mutants compared to the wild-type fish (Fig. 8C, C', 8D and 8D'). In contrast, at 19 months increases of erythrophores, iridophores and xanthophores were observed in the mutants (Fig. 8G, G', 8H and 8H') compared to the wild-type fish (Fig. 8E, E', 8F and 8F'). Additionally, wild-type fish had fewer erythrophores, with less carotenoid pigmentation, spread randomly in the dorsal scales (Fig. 8I), while mutants had more erythrophores, with more carotenoid pigmentation (Fig. 8J).

Quantification of the pigment cells revealed significantly higher number of xanthophores in dorsal scales of *hps4*$^{-/-}$ mutants at 6 months, and significantly higher number of erythrophores in dorsal scales of *hps4*$^{-/-}$ mutants at 19 months than in wild-type fish (Fig. 8K-8L). The number of erythrophores in the aged mutants was 2–3 times higher than that in wild-type fish (Fig. 8L).

4. Discussion

4.1. Disruption of HPS4 led to a silver-white body color in Nile tilapia

Body color is fundamental to the economic value of domesticated animals, as people naturally associate their color with health, ornamental or nutritional value and even meat quality (Jiang et al., 2014; Zhang et al., 2017b; Lehnert et al., 2019; Maoka, 2020; Widjaja-Adhi and Golczak, 1865; Wu et al., 2022). In teleosts, many studies have been conducted to improve color traits, including studies in zebrafish (Patterson and Parichy, 2019), medaka (Nagao et al., 2018; Fang et al., 2018), carp (Chen et al., 2018; Mandal et al., 2019; Du et al., 2021), crucian carp (Xu et al., 2015; Liu et al., 2019) and even tilapia (McAndrew et al., 1988; Huang et al., 1996; Wang et al., 2021). The hundreds of color mutants in zebrafish provid excellent materials for the pet fish market and the study of mechanisms of color patterning (Kelsh et al., 1996; Singh and Nüsslein-Volhard, 2015; Patterson and Parichy, 2019). In farmed fish, body color also directly determines economic value. For example, in tilapia, naturally red mutants were preferred by customers than the black wild-type fish in some countries and regions around the world (McAndrew et al., 1988; Huang et al., 1996; Zhu et al., 2016; Wang et al., 2020). Disruption of *tyr* in red tilapia results in a red strain without black patches (Lu et al., 2022). Recently, we developed Nile tilapia as an excellent model for studies of fish pattern development (Wang et al., 2021). In this study, we engineered a *hps4* mutant line using CRISPR/Cas9 in Nile tilapia. The mutants displayed a silver-white body color and more carotenoids pigmentation in the adult mutants, without bars, inter-bars or any black patches. A previous study suggested that *hps4* is the locus for a natural albino of channel catfish through GWAS mapping (Li et al., 2017), but to our knowledge, this is the first report of artificial mutation of *hps4* in teleosts. Increasing amount of erythrophores in the reddish-silver-white *hps4* adult mutants might help them to be favored by the customers, as they not only showed an attractive global color patterning but also may be enriched in carotenoids. It should be not ignored that even though body color has also been acknowledged to be linked with growth rates in vertebrates (Hou and Pavan, 2008), so far, there is no evidence that there is a significant difference between the growth rate of the silver-white tilapia mutants and wild-type fish. However, during feeding and breeding, we found that these silver-white mutants preferred to stay in areas with weak light, which suggested that the color mutants may be more sensitive to light than the wild-type fish. Additionally, mutants of the F3 generation displayed a stable silver-white body color.

4.2. HPS4 was indispensable for melanin biosynthesis in tilapia

Pigment-containing organelles belong to a larger class of cellular organelles, i.e., lysosome-related organelles (LROs). Melanosomes are the most widely studied LROs (Dell'Angelica et al., 2000; Dell'Angelica, 2004). As one of the key genes in directing melanosome biosynthesis, *hps4* has been suggested to be fundamental for the melanophore stability in humans (Bachli et al., 2004), mice (Suzuki et al., 2002), and even teleosts like channel catfish (Li et al., 2017). Disruption of another *hps* family gene, *hps5,* in zebrafish led to significant hypo-pigmentation across the whole fish, which showing a “snow-white” phenotype (but still with many hypo-pigmented melanophores) in larvae (Daly et al., 2013). Another study conducted on stickleback suggested that a naturally mutation of *hps5* locus was related to the *casper*-like phenotype, indicated by a loss of black pigmentation and iridescent color in body surface, eyes and even inner organs (Hart and Miller, 2017). In this study, we found that *hps4* was important for melanin biosynthesis in tilapia, as the *hps4*$^{-/-}$ mutants had no pigmented melanophores or melanin. However, as the mutants were still detected with some banding in the dorsal, anal and caudal fins in aged mutants, we deduced that some melanophores were probably still in the fins, while just not pigmented. This situation was similar to the studies in zebrafish *tyr* mutants, in which melanophores were found to be still in the mutants as *mitfa* (the most important marker gene for melanophore differentiation) staining was detected (Taylor et al., 2011). It should be mentioned that in the previous studies of transcriptome data of other body color mutants including common carp, tilapia, crucian carp and rainbow trout, etc., the key genes of canonical melanin synthesis pathway were always significantly down-regulated in mutants with insufficient or no melanosome (a

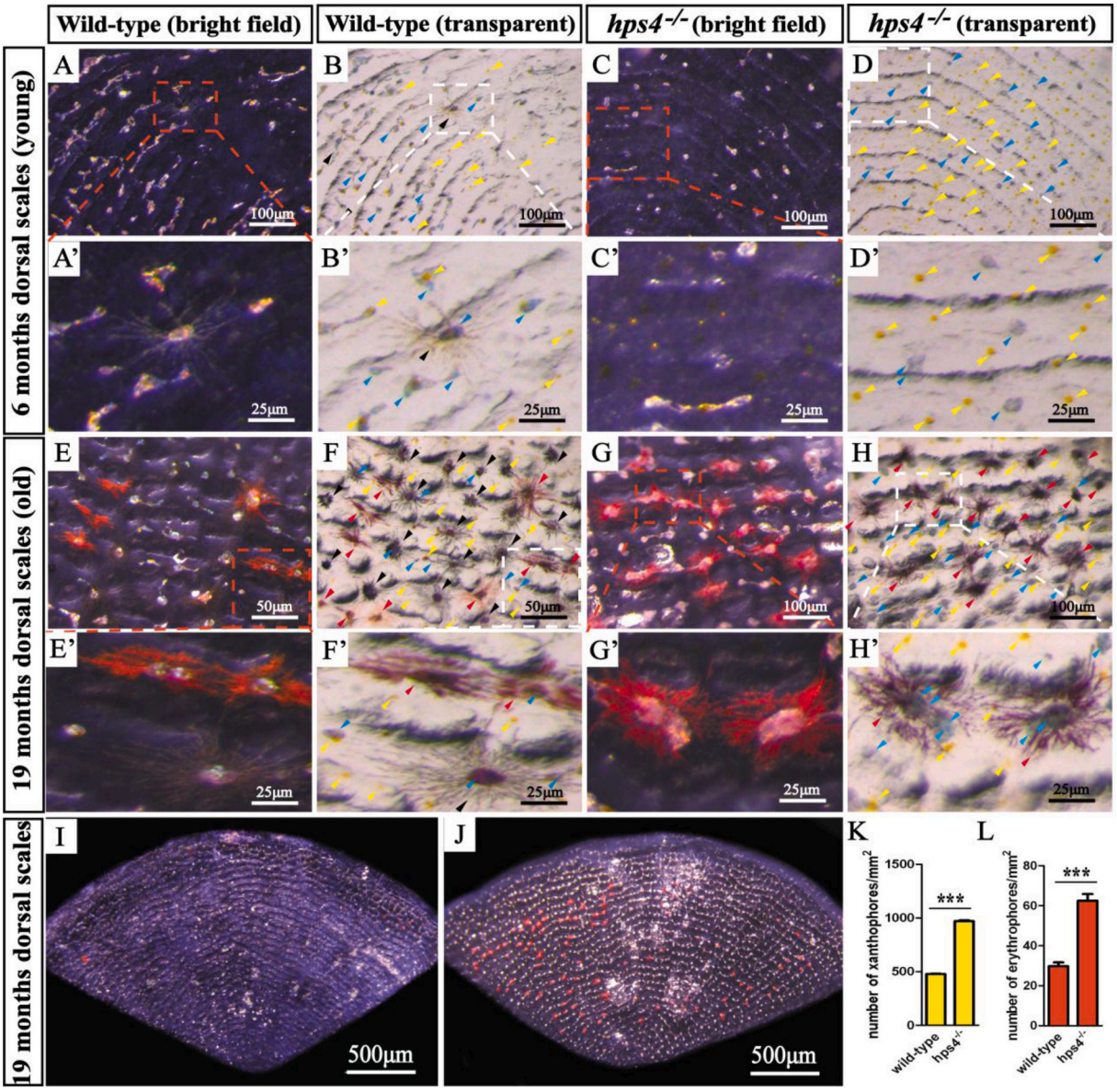

Fig. 8. Increased white iridophores, xanthophores/erythrophores and no melanophores were observed in scales of the young (6 months) and old (19 months) *hps4*$^{-/-}$ mutants.

A, A', B and B′: Scales from the wild-type fish at 6 months displayed many xanthophores (yellow arrow heads) and many colorful iridophores (blue arrow heads) covering the main bodies of the melanophores (black arrow heads). C, C′, D and D′: The scales from the mutants at 6 months displayed many big iridophore-composed round spots and increased xanthophores, while no pigmented melanophores were observed. E, E', F and F′: Scales from the wild-type fish at 19 months displayed many xanthophores and many colorful iridophores covering the main bodies of the melanophores and erythrophores. G, G', H and H′: Scales from the mutants at 19 months displayed increased erythrophores and big white iridophore-composed round spots, with some of them covering the main body of erythrophores. In contrast, no pigmented melanophores were observed. I, J, L: Scales from the wild-type fish (I) at 19 months displayed significantly fewer erythrophores than scales from the mutants (J). Besides, erythrophores in the scales from the wild-type fish spread randomly, while those from the mutants were restricted in a specific area. K: Significantly higher number of xanthophores was detected in scales from the mutants at 6 months. L: Significantly higher number of erythrophores was detected in scales from the mutants at 19 months. Data in K and L are expressed as mean ± SD ($n = 5$). Differences in the data between the wild-type fish and mutants were tested by two-tailed Student's *t*-test, $^{***}P < 0.001$, $^{**}P < 0.01$, $^{*}P < 0.05$, ns: not significant. (For interpretation of the references to color in this figure legend, the reader is referred to the web version of this article.)

pigment granule formed from a protein that appears black, gray, or even brown) (Jiang et al., 2014; Zhu et al., 2016; Zhang et al., 2017a, 2017b; Wu et al., 2022). Besides, the protein levels of Mitfa, Tyr and Dct in red crucian carp were also significantly lower than in wild-type fish (Zhang et al., 2017a). Additionally, a previous knock-out study of *tyr* in crucian carp also suggested that the expression profile of other genes in melanin synthesis and regulatory pathways were significantly decreased in the white mutants (Liu et al., 2019). However, we did not perform skin transcriptome analysis, Western-blot or other follow-up analysis of the mutants. As we detected no melanosomes in the melanin-free skin of the silver-white mutants (5 months) by melanin quantification analysis, we predicted that the expression levels of other genes in melanin synthesis and regulatory pathways also decreased or silenced.

4.3. Modeling on the effects of *hps4* mutation on pigment cells relative abundance, melanin biosynthesis and LROs-pigment development in Nile tilapia

The *hps4* mutants showed significant hypo-pigmentation across the whole fish (trunk, fins, RPE and iris), which led to a complete silver-white tilapia. Strikingly, with the development of the mutants, a reddish-silver-white body color was detected for the old fish due to accumulation of carotenoids pigmentation (Fig. 9A). The wild-type fish had melanophores across the whole body, fins and eyes, with sufficient melanin. Iridophores frequently associate with the main body of melanophores, especially in the skin and scales. However, in *hps4* albino mutants lacking melanophores, iridophores increased explosively and spread widely, no longer gathered near the main body of melanophores or showing blue/purple/red colors. Instead, they gathered as a big round spots and showed a uniform white color, which finally led to a complete silver-white body color (Fig. 9B).

The HPS/BLOC gene family is fundamental for directing melanin biosynthesis and melanosome pH levels. Previous studies suggested that *hps5* participates in the zebrafish melanosome phase transition (from phase I to phase II, and phase II to phase III), as the *hps5* mutants (BLOC2) showed significant hypo-pigmentation in melanophores and the whole larvae (Daly et al., 2013). The *hps4* natural mutation in channel catfish leads to dysfunction of BLOC3 complex, which in turn, leads to a defect in Rab GTPase activation and recruitment, and thus disrupts melanin biosynthesis (Li et al., 2017). In this study, we found that *hps4* (BLOC3) is a major factor in directing melanin biosynthesis from lysosome to phase I melanosome (Fig. 9C). As we detected almost no melanophores and melanin in the mutants, while detecting a vast increase of white iridophores and white iridophore-composed big round spots.

It has been well documented that different kinds of pigment cells arise by alternative differentiation of LROs, and the LROs were able to transition into organelles producing different kinds of pigment: melanosomes producing melanin, xanthosomes producing pteridine, erythrosomes accumulating carotenoids and iridosomes synthesizing guanine, to determine the color patterning (pigment granules development) of melanophores, xanthophores, erythrophores and iridophores, respectively (Ullate-Agote et al., 2020). Additionally, in this study, a significant increase of carotenoids/pteridine pigmentation and erythrophores/xanthophores were detected in the older reddish-silver-white mutants, which was slight different from the complete silver-white young fish, suggesting that lysosomes originally destined to synthesize melanosomes probably latter developed as the basis of LROs in other

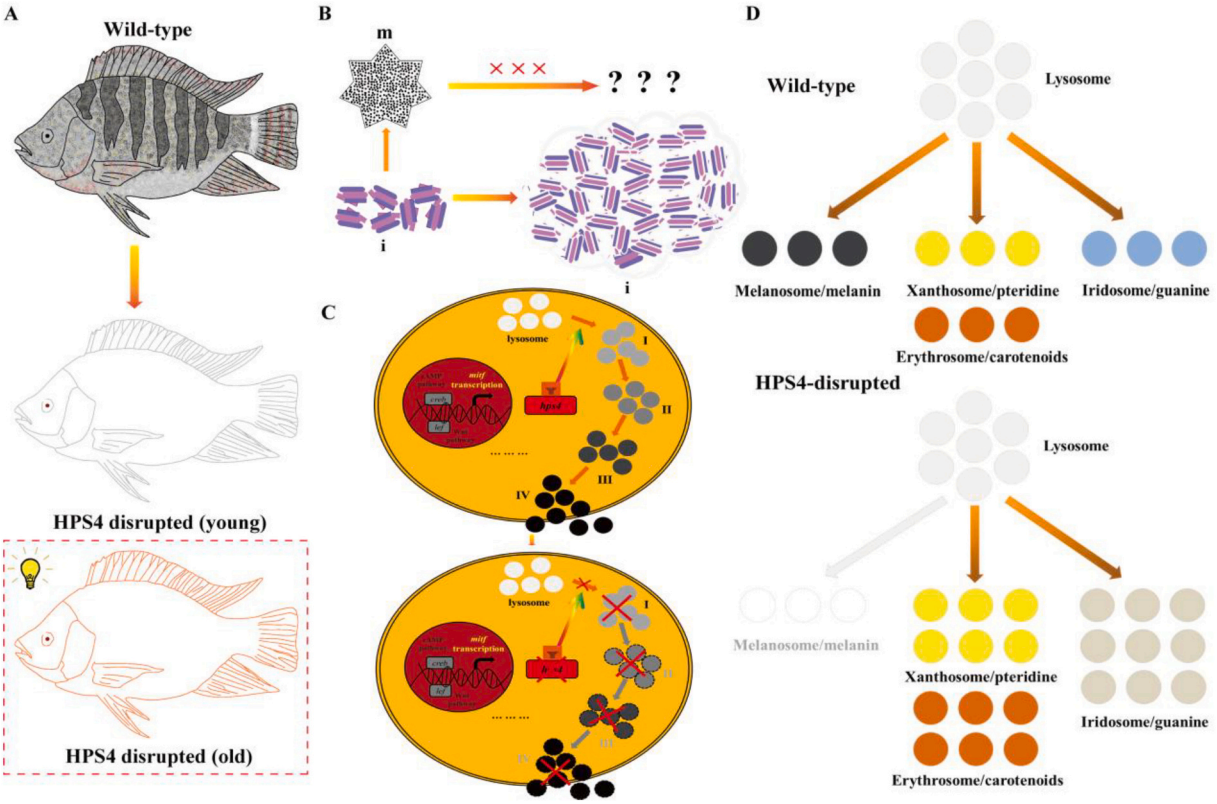

Fig. 9. Proposed model of the phenotype of *hps4*$^{-/-}$ mutants and function of HPS4 in melanin biosynthesis and pigment development in Nile tilapia.
A: Disruption of *hps4* resulted in silver-white body color and dark red eyes in Nile tilapia. Additionally, the old sexually matured fish were detected with a reddish-silver-white body color as an accumulation of erythrophores/carotenoids. B: Disruption of *hps4* resulted in absence of melanophores and melanin in the mutants, suggesting that *hps4* was fundamental for melanophores (both NCCs-derived and optic cup-derived melanophore) survival and melanin biosynthesis. In wild-type fish, iridophores like the melanophores as reflected by the attachment of iridophores on the main body of the melanophores. However, in the mutants, an increase of iridophores was detected. C: Schematic view of melanin biosynthesis. *Mitf* as the key transcription factor for melanogenesis is responsible for cis-directing the *mitf*-axis down-stream genes such as *hps4*. There are four phases for melanin biosynthesis, *hps4* was fundamental for lysosome to phase I melanosome transition in tilapia. In HPS4-disrupted Nile tilapia, the lysosome to phase I melanosome process in melanin biosynthesis was blocked, as no melanosomes at any phases were observed. D: In wild-type fish, LROs (lysosome-related organelles) were able to be developed into melanosome/melanin, xanthosome/pteridine, erythrosome/carotenoids and iridosome/guanine, thus four kinds of fully functional pigment cells were detected. However, in the HPS4-disrupted mutants, the LROs originally destined to synthesize melanosomes were high likely to be latter developed as pigments of other pigment cells, resulted in an increase of iridophores, xanthophores and erythrophores in the mutants, which gave the whole fish a reddish-silver-white body color. *Hps4* played a fundamental role in LROs-pigments development, melanophores survival and melanin biosynthesis. m, melanophores; i, iridophores. (For interpretation of the references to color in this figure legend, the reader is referred to the web version of this article.)

types of pigment cells like iridophores, xanthophores and even erythrophores in the HPS4-disrupted mutants (Fig. 9D). However, it is possible that some of the xanthophores and erythrophores were masked by melanophores in the wild-type fish. The critical transcription factor *mitf* has been acknowledged to be fundamental for melanogenesis and even lysosome formation in mice and human (Hou and Pavan, 2008). Three *mitf*-binding sites predicted in *hps4* promoter suggested that it is probably regulated by *mitf*, which was further supported by the similar phenotype observed in *mitfa*$^{-/-}$ mutants in zebrafish and *hps4*$^{-/-}$ mutants in tilapia.

4.4. The appearance of macro-melanophores on the head was independent of hps4 in tilapia

Even though disruption of HPS4 led to a complete silver-white body color in tilapia, and no melanophores or melanin were detected since 30 dpf, the mutants were detected with melanophores only on top of the head at 12 dpf, suggested that a subgroup of melanophores were independent of *hps4*. Additionally, the number of remaining melanophores was much less than the wild-type fish and the melanophores were much smaller in size than the wild-type fish. In our previous studies, several waves of melanophore differentiation (normal melanophores in yolk sac, trunk and fins, and macro-melanophores in head and trunk, respectively) were detected during tilapia development (Wang et al., 2021). The melanophores on top of the head were mainly macro-melanophores in wild-type fish at 12 dpf, while the remaining macro-melanophores became tiny spots in the *hps4*$^{-/-}$ mutants at 12 dpf, suggesting that *hps4* was required for maintaining the size of macro-melanophores. With further development, no melanophores nor melanin were detected anymore, suggesting that melanin biosynthesis in all the melanophores (including the macro-melanophores) was depended on *hps4*, and the tiny "macro-melanophores" detected in the top head of the mutants at early 12 dpf were probably broken down and eliminated during development.

4.5. RPE pigmentation reflected both blood capillary and carotenoids in the hps4$^{-/-}$ mutants, and was different from that of the wild-type fish or usual ocular albino

The natural *hps4* mutants in channel catfish display a pink body and eyes, thus *hps4* was supposed to be closely linked with ocular albinism in catfish (Li et al., 2019). In tilapia and other cichlids, several albino mutants have been created by disruption of the melanogenesis genes, such as *tyr*, *slc24a5*, *slc45a2*, and significant ocular albinism phenotypes were detected in them (Wang et al., 2021; Li et al., 2021; Pandey et al., 2021; Segev-Hadar et al., 2021; Lu et al., 2022). It should be highlighted that all those albinos displayed non-pigmented RPE that was easy to be distinguished from the lateral view by naked eyes. However, in this study, we found that it was difficult to distinguish the color of eyes between *hps4*$^{-/-}$ mutants and the wild-type fish, especially at the adult stage. Additionally, the RPE color was also different from the *hps4*$^{-/-}$ channel catfish mutants as catfish mainly contain melanin/melanophores. In the very early developmental stages (3, 5, 7 and 12 dpf), the RPE in the tilapia *hps4*$^{-/-}$ mutants were pink in coloration, as a reflection of capillary network. However, in later stages (from 30 dpf), RPE coloration of the mutants was gradually difficult to distinguish from the wild-type fish, due to the accumulation of carotenoids. It has been well documented that carotenoids are rich in the eyes of teleosts (Du et al., 2021) and other vertebrates like birds and turtles (Twyman et al., 2016). Genes responsible for carotenoids absorption and transportation are highly expressed in the RPE. In tilapia, carotenoids are also critical for body color formation, as demonstrated by specific gene knock out (Wang et al., 2021). To our knowledge, the traditional view on *hps* family members is that they are critical for melanogenesis, and it has rarely been reported that carotenoids were regulated by *hps* family members. The RPE of tilapia *hps4*$^{-/-}$ adult mutants displayed deep red color due to the increased red carotenoids pigmentation overriding the coloration of the capillary network. This was consistent with the increasing amounts of reddish coloration (carotenoids-rich erythrophores) in whole trunk, fins and even iris. However, whether the carotenoids were significantly increased in eyes of the tilapia mutants remains to be investigated.

5. Conclusion

Body color is an important economic trait in teleosts. In this study, we engineered a new silver-white tilapia by disrupting *hps4* in Nile tilapia with CRISPR/Cas9. Phenotype analysis of the mutants confirmed the role of *hps4* in directing melanogenesis and melanophore survival. Additionally, *hps4* was also found to be closely linked with LROs-pigment development by directing iridophore, xanthophore and erythrophore relative abundance. To our knowledge, this is the first report on *hps4* mutation in vertebrates, which provide a new model for studies of *hps4* function. Besides, the silver-white tilapia created by us may also serve the aquaculture industry as an excellent ornamental and food fish.

Supplementary data to this article can be found online at https://doi.org/10.1016/j.aquaculture.2022.738420.

Author contributions

DW acquired the funding, designed research, conducted investigation and administrated the project; CW created the mutants; TDK suggested strategies for phenotype analysis; CW, BL and XJ participated in methology application and software analysis; CW and DW curated the data; CW, DW and TDK wrote the original draft; wrote, reviewed and edited the finalized manuscript.

CRediT authorship contribution statement

Chenxu Wang: Software, Formal analysis, Validation, Data curation, Investigation, Resources, Writing – original draft, Writing – review & editing, Visualization. **Thomas D. Kocher:** Methodology, Writing – original draft, Writing – review & editing. **Baoyue Lu:** Software, Formal analysis, Validation. **Jia Xu:** Software, Formal analysis, Validation. **Deshou Wang:** Conceptualization, Investigation, Data curation, Writing – original draft, Writing – review & editing, Supervision, Project administration, Funding acquisition.

Declaration of Competing Interest

The authors declare that they have no known competing financial interests or personal relationships that could have appeared to influence the work reported in this paper.

Acknowledgements

This work was supported by grants 31872556, 31861123001 and 31630082 from the National Natural Science Foundation of China; grants cstc2021ycjh-bgzxm0024 and CQYC201903173 from the Chongqing Science and Technology Bureau. We thank Hesheng Xiao, Feilong Wang and Zhuo Yang for technical support and experimental fish caring.

References

Bachli, E.B., Brack, T., Eppler, E., Stallmach, T., Trueb, R.M., Huizing, M., et al., 2004. Hermansky–Pudlak syndrome type 4 in a patient from Sri Lanka with pulmonary fibrosis. Am. J. Med. Genet. A 127A, 201–207.

Brawand, D., Wagner, C.E., Li, Y.I., Malinsky, M., Keller, I., Fan, S., et al., 2014. The genomic substrate for adaptive radiation in African cichlid fish. Nature 513, 375–381.

Chen, H., Wang, J., Du, J., Si, Z., Yang, H., Xu, X., et al., 2018. ASIP disruption via CRISPR/Cas9 system induces black patches dispersion in Oujiang color common carp. Aquaculture 498, 230–235.

Daly, C.M., Willer, J., Gregg, R., Gross, J.M., 2013. *snow white*, a zebrafish model of Hermansky-Pudlak Syndrome type 5. Genetics 195 (2), 481–494.
Dell'Angelica, E.C., 2004. The building BLOC(k)s of lysosomes and related organelles. Curr. Opin. Cell Biol. 16, 458–464.
Dell'Angelica, E.C., Mullins, C., Caplan, S., Bonifacino, J.S., 2000. Lysosome-related organelles. Federat. Am. Soc. Exp. Biol. J. 14, 1265–1278.
Dong, C., Wang, H., Xue, L., Dong, Y., Yang, L., Fan, R., et al., 2012. Coat color determination by miR-137 mediated down-regulation of microphthalmia-associated transcription factor in a mouse model. RNA 18 (9), 1679–1686.
Du, J., Chen, H., Mandal, B.K., Wang, J., Wang, C., 2021. HDL receptor/scavenger receptor B1-*Scarb1* and *Scarb1*-like mediate the carotenoid-based red coloration in fish. Aquaculture 545 (2).
Fang, J., Chen, T., Pan, Q., Wang, Q., 2018. Generation of albino medaka (*Oryzias latipes*) by CRISPR/Cas9. J. Exp. Zool. B Mol. Dev. Evol. 330 (4), 242–246.
Fujii, R., 2000. The regulation of motile activity in fish chromatophores. Pigment Cell Res. 13, 300–319.
Gerondopoulos, A., Langemeyer, L., Liang, J.R., Linford, A., Barr, F.A., 2012. BLOC-3 mutated in Hermansky-Pudlak syndrome is a Rab32/38 guanine nucleotide exchange factor. Curr. Biol. 22, 2135–2139.
Hart, J.C., Miller, C.T., 2017. Sequence-based mapping and genome editing reveal mutations in stickleback *hps5* cause oculocutaneous albinism and the *casper* phenotype. Genes Genom. Genet. (Bethesda) 7 (9), 3123–3131.
Hendrick, L.A., Carter, G.A., Hilbrands, E.H., Heubel, B.P., Schilling, T.F., Pabic, P.L., 2019. Bar, stripe and spot development in sand-dwelling cichlids from Lake Malawi. Evodevo 10, 18.
Hoekstra, H.E., 2006. Genetics, development and evolution of adaptive pigmentation in vertebrates. Heredity (Edinb) 97 (3), 222–234.
Hou, L., Pavan, W.J., 2008. Transcriptional and signaling regulation in neural crest stem cell-derived melanocyte development: do all roads lead to *Mitf*? Cell Res. 18 (12), 1163–1176.
Huang, C.M., Chang, S.L., Chen, H.J., Liao, I.C., 1996. Single gene inheritance of red body coloration in Taiwanese red tilapia. Aquaculture 74, 227–232.
Huizing, M., Hess, R., Dorward, H., Claassen, D.A., Helip-Wooley, A., Kleta, R., et al., 2004. Cellular, molecular and clinical characterization of patients with Hermansky-Pudlak syndrome type 5. Traffic 5 (9), 711–722.
Huizing, M., Helip-Wooley, A., Westbroek, W., Gunay-Aygun, M., Gahl, W.A., 2008. Disorders of lysosome-related organelle biogenesis: clinical and molecular genetics. Annu. Rev. Genomics Hum. Genet. 9, 359–386.
Ito, S., Wakamatsu, K., 2011. Human hair melanins: what we have learned and have not learned from mouse coat color pigmentation. Pigment Cell Melan. Res. 24 (1), 63–74.
Jiang, Y., Zhang, S., Xu, J., Feng, J., Mahboob, S., Al-Ghanim, K.A., et al., 2014. Comparative transcriptome analysis reveals the genetic basis of skin color variation in common carp. PLoS One 9 (9), e108200.
Kelsh, R.N., 2004. Genetics and evolution of pigment patterns in fish. Pigment Cell Res. 17 (4), 326–336.
Kelsh, R.N., Brand, M., Jiang, Y.J., Heisenberg, C.P., Lin, S., Haffter, P., et al., 1996. Zebrafish pigmentation mutations and the processes of neural crest development. Development 123, 369–389.
Kocher, T.D., 2004. Adaptive evolution and explosive speciation: the cichlid fish model. Nat. Rev. Genet. 5, 288–298.
Kratochwil, C.F., Liang, Y., Gerwin, J., Woltering, J.M., Urban, S., Henning, et al., 2018. Agouti-related peptide 2 facilitates convergent evolution of stripe patterns across cichlid fish radiations. Science 362 (6413), 457–460.
Lehnert, S.J., Christensen, K.A., Vandersteen, W.E., Sakhrani, D., Pitcher, T.E., Heath, J. W., et al., 2019. Carotenoid pigmentation in salmon: variation in expression at BCO2-l locus controls a key fitness trait affecting red coloration. Proc. R. Soc. B Biol. Sci. 286 (1913), 20191588.
Li, Y., Geng, X., Bao, L., Elaswad, A., Huggins, K.W., Dunham, R., et al., 2017. A deletion in the Hermansky-Pudlak syndrome 4 (*Hps4*) gene appears to be responsible for albinism in channel catfish. Mol. Gen. Genomics. 292 (3), 663–670.
Li, C.Y., Steighner, J.R., Sweatt, G., Thiele, T.R., Juntti, S.A., 2021. Manipulation of the *Tyrosinase* gene permits improved CRISPR/Cas editing and neural imaging in cichlid fish. Sci. Rep. 11 (1), 15138.
Liang, Y., Gerwin, J., Meyer, A., Kratochwil, C.F., 2020. Developmental and cellular basis of vertical bar color patterns in the East African cichlid fish *Haplochromis latifasciatus*. Front. Cell Dev. Biol. 8, 62.
Liu, Q., Qi, Y., Liang, Q., Song, J., Liu, J., Li, W., et al., 2019. Targeted disruption of tyrosinase causes melanin reduction in *Carassius auratus cuvieri* and its hybrid progeny. Sci. China Life Sci. 62 (9), 1194–1202.
Lu, B., Liang, G., Xu, M., Wang, C., Tan, D., Tao, W., et al., 2022. Production of all male amelanotic red tilapia by combining MAS-GMT and *tyrb* mutation. Aquaculture 546, 737327.
Mandal, B.K., Chen, H., Si, Z., Hou, X., Yang, H., Xu, X., et al., 2019. Shrunk and scattered black spots turn out due to MC1R knockout in a white-black Oujiang color common carp (*Cyprinus carpio var.color*). Aquaculture 734822.
Maoka, T., 2020. Carotenoids as natural functional pigments. J. Nat. Med. 74 (1), 1–16.
McAndrew, B.J., Roubal, F.R., Roberts, R.J., Bullock, A.M., Mcewen, I.M., 1988. The genetics and histology of red, blond and associated colour variants in *Oreochromis niloticus*. Genetica 76, 127–137.
Nagao, Y., Takada, H., Miyadai, M., Adachi, T., Seki, R., Kamei, Y., et al., 2018. Distinct interactions of *Sox5* and *Sox10* in fate specification of pigment cells in medaka and zebrafish. PLoS Genet. 14 (4), e1007260.
Nguyen, T., Novak, E.K., Kermani, M., Fluhr, J., Peters, L.L., Swank, R.T., et al., 2002. Melanosome morphologies in murine models of Hermansky-Pudlak syndrome reflect blocks in organelle development. J. Investig. Dermatol. 119, 1156–1164.
O'Quin, C.T., Drilea, A.C., Conte, M.A., Kocher, T.D., 2013. Mapping of pigmentation QTL on an anchored genome assembly of the cichlid fish, *Metriaclima zebra*. BMC Genomics 14, 287.
Pandey, D., Matsubara, T., Saito, T., Kazeto, Y., Gen, K., Sakuma, T., et al., 2021. TALEN-mediated gene editing of *slc24a5* (solute carrier family 24, member 5) in kawakawa, *Euthynnus affinis*. J. Mar. Sci. Eng. 9, 1378.
Patterson, L.B., Parichy, D.M., 2019. Zebraish pigment pattern formation: insights into the development and evolution of adult form. Annu. Rev. Genet. 53, 505–530.
Protas, M.E., Patel, N.H., 2008. Evolution of coloration patterns. Annu. Rev. Cell Dev. Biol. 24, 425–446.
Raposo, G., Tenza, D., Murphy, D.M., Berson, J.F., Marks, M.S., 2001. Distinct protein sorting and localization to premelanosomes, melanosomes, and lysosomes in pigmented melanocytic cells. J. Cell Biol. 152 (4), 809–824.
Santos, M.E., Braasch, I., Boileau, N., Meyer, B.S., Sauteur, L., Böhne, A., et al., 2014. The evolution of cichlid fish egg-spots is linked with a *cis*-regulatory change. Nat. Commun. 5, 5149.
Schneider, C.A., Rasband, W.S., Eliceiri, K.W., 2012. NIH image to ImageJ: 25 years of image analysis. Nat. Methods 9 (7), 671–675.
Segev-Hadar, A., Slosman, T., Rozen, A., Sherman, A., Cnaani, A., Biran, J., 2021. Genome editing using the CRISPR-Cas9 system to generate a solid-red germline of Nile tilapia (*Oreochromis niloticus*). CRISPR J. 4 (4), 583–594.
Singh, A.P., Nüsslein-Volhard, C., 2015. Zebrafish stripes as a model for vertebrate colour pattern formation. Curr. Biol. 25 (2), R81–R92.
Sköld, H.N., Aspengren, S., Cheney, K.L., Wallin, M., 2016. Fish chromatophores-from molecular motors to animal behavior. Int. Rev. Cell Mol. Biol. 321, 171–219.
Sun, Y.L., Jiang, D.N., Zeng, S., Hu, C.J., Ye, K., Yang, C., et al., 2014. Screening and characterization of sex-linked DNA markers and marker-assisted selection in the Nile tilapia (*Oreochromis niloticus*). Aquaculture 433, 19–27.
Suzuki, T., Li, W., Zhang, Q., Karim, A., Novak, E.K., Sviderskaya, E.V., et al., 2002. Hermansky-Pudlak syndrome is caused by mutations in HPS4, the human homolog of the mouse light-ear gene. Nat. Genet. 30, 321–324.
Taylor, K.L., Lister, J.A., Zeng, Z., Ishizaki, H., Anderson, C., Kelsh, R.N., et al., 2011. Differentiated melanocyte cell division occurs in vivo and is promoted by mutations in *Mitf*. Development 138 (16), 3579–3589.
Twyman, H., Valenzuela, N., Literman, R., Andersson, S., Mundy, N.I., 2016. Seeing red to being red: conserved genetic mechanism for red cone oil droplets and co-option for red coloration in birds and turtles. Proc. Biol. Sci. R. Soc. 283 (1836), 20161208.
Ullate-Agote, A., Burgelin, I., Debry, A., Langrez, C., Montange, F., Peraldi, R., et al., 2020. Genome mapping of a LYST mutation in corn snakes indicates that vertebrate chromatophore vesicles are lysosome-related organelles. Proc. Natl. Acad. Sci. U. S. A. 117 (42), 26307–26317.
Wang, L., Luo, M., Yin, H., Zhu, W., Fu, J., Dong, Z., 2020. Effects of background adaptation on the skin color of Malaysian red tilapia. Aquaculture 521, 735061.
Wang, C., Lu, B., Li, T., Liang, G., Xu, M., Liu, X., et al., 2021. Nile tilapia: a model for studying teleost color patterns. J. Hered. 112 (5), 469–484.
Wang, C., Xu, J., Kocher, T.D., Li, M., Wang, D., 2022. CRISPR knockouts of *pmela* and *pmelb* engineered a golden tilapia by regulating relative pigment cell abundance. J. Hered. esac018. Online ahead of print.
Wasmeier, C., Hume, A.N., Bolasco, G., Seabra, M.C., 2008. Melanosomes at a glance. J. Cell Sci. 121, 3995–3999.
Wei, M.L., 2006. Hermansky-Pudlak syndrome: a disease of protein trafficking and organelle function. Pigment Cell Res. 19 (1), 19–42.
Widjaja-Adhi, M.A.K., Golczak, M., 1865. The molecular aspects of absorption and metabolism of carotenoids and retinoids in vertebrates. Biochim. Biophys. Acta Mol. Cell Biol. Lipids 2020 (11), 158571.
Wu, S., Huang, J., Li, Y., Zhao, L., Liu, Z., 2022. Analysis of yellow mutant rainbow trout transcriptomes at different developmental stages reveals dynamic regulation of skin pigmentation genes. Sci. Rep. 12 (1), 256.
Xu, W., Tong, G.X., Geng, L.W., Jiang, H.F., 2015. Body color development and genetic analysis of hybrid transparent crucian carp (*Carassius auratus*). Genet. Mol. Res. 14 (2), 4399–4407.
Yamaguchi, Y., Hearing, V.J., 2009. Physiological factors that regulate skin pigmentation. Biofactors 35, 193–199.
Yan, B., Liu, B., Zhu, C.D., Li, K.L., Yue, L.J., Zhao, J.L., et al., 2013. microRNA regulation of skin pigmentation in fish. J. Cell Sci. 126 (15), 3401–3408.
Zhang, Y., Liu, J., Fu, W., Xu, W., Zhang, H., Chen, S., et al., 2017a. Comparative transcriptome and DNA methylation analyses of the molecular mechanisms underlying skin color variations in Crucian carp (*Carassius carassius L.*). BMC Genet. 18, 95.
Zhang, Y., Liu, J., Peng, L., Ren, L., Zhang, H., Zou, L., et al., 2017b. Comparative transcriptome analysis of molecular mechanism underlying gray-to-red body color formation in red crucian carp (*Carassius auratus, red var.*). Fish Physiol. Biochem. 43 (5), 1387–1398.
Zhu, W., Wang, L., Dong, Z., Chen, X., Song, F., Liu, N., et al., 2016. Comparative transcriptome analysis identifies candidate genes related to skin color differentiation in red tilapia. Sci. Rep. 6, 31347.